A zero-electrical-power Silicon Photonic Ternary Content Addressable Memory Bank

S. Simos[(1)], T. Moschos[(1)], S. Kovaios[(1)], A. Tsakyridis[(1)], M. Moralis-Pegios[(1)], I. Johnson[(2)], T. Rangarajan[(2)], T. D. Bucio[(2)], J. Gates[(2)], F. Gardes[(2)] and N. Pleros[(1)]

[(1)] Department of Informatics, Center for Interdisciplinary Research & Innovation, AUTH, Thessaloniki, Greece
[(2)] Optoelectronics Research Centre, University of Southampton, Southampton, SO17 1BJ, United Kingdom
e-mail address: simostyl@csd.auth.gr

Abstract: We demonstrate a silicon photonic 4×9 WDM ternary content addressable memory bank, that consumes zero-electrical power. Successful TCAM operation for 2-bit optical words at 20 Gb/s is experimentally presented.

1. Introduction

Content addressable memories (CAMs) are indispensable building blocks in high-performance computing systems, enabling parallel search operations in a single clock cycle [1]. Their use spans from networking and database management to security and emerging AI workloads, where ultrafast and energy-efficient memory access is essential [2]. Yet, despite decades of development, electronic CAMs/ternary CAMs (TCAMs) remain constrained by a fundamental trade-off: increasing the operating frequency inevitably results in prohibitively high-power consumption, since the intrinsic size and energy advantages of electronics are offset by the RC parasitic limits of on-chip interconnects [3]. This limitation, which has stalled progress towards next-generation computing performance, is now being challenged by the recent emergence of photonic implementations, which capitalize on the ultrafast response and wide bandwidth of optics to achieve far superior speeds. [4][6]. However, current photonic CAMs have consistently required significant power, mainly due to continuous biasing, thermal tuning, or the use of semiconductor optical amplifiers (SOAs) [4],[7], posing a direct conflict between operational speed and power efficiency.

In this work, we break this barrier by demonstrating, for the first time, a wavelength division multiplexing (WDM)-empowered silicon photonic TCAM bank with the highest memory bank dimensions in the photonic domain (4×9) that operates with 2-bit optical words at 20 Gb/s and consumes zero electrical power. Our approach leverages a CMOS compatible process that allows the modification of the refractive index of the n-rich Si_3N_4 material [8], that can be permanently modified by high-energy ultraviolet (UV) laser exposure [9], in a wafer scale. Once modified, the refractive index remains stable, allowing the memory to operate with zero static power while preserving full transparency to the bit rate. This enables non-volatile programming of the CAM states without the need of biasing or thermal tuning in our architecture. Successful experimental operation of the WDM CAM matchline is demonstrated for 2-bit optical words when compared with all 9 different stored words in the respective 9 memory columns. This breakthrough establishes a new class of high-speed, non-volatile, and energy-free CAMs that decisively outperform existing electronic and photonic alternatives.

2. Zero-power Optical Ternary Content Addressable Memory architecture

The architecture of a single WDM TCAM cell is illustrated in Fig. 1(a), alongside a functional representation of its operation for all three cases of stored information i.e. “0”, “1” and the ternary “X”. The search information and it’s complementary value (Bit, $\overline{Bit}$) are encoded via NRZ binary signals into two different wavelengths (λ_1 and λ_2), that subsequently propagate through two different Mach Zehnder interferometers (MZIs), respectively. By controlling the phase difference between the two MZI branches, the propagating signal can either experience significant attenuation, defined as the “OFF” state, or propagate through the MZI without attenuation, defined as the “ON” state. In our specific, implementation the phase difference is controlled through a UV-enabled post-processing step, that enables transition between the two states. The signals are then combined in a symmetric splitter, with the resulting multi-wavelength signal injected into a photodiode (PD) for incoherent addition. In this way, the electrical signal emerging at the PD represents the dot-product between the search and stored vectors. Exemplary, a TCAM cell that is configured in the [ON,OFF] state, corresponding to the stored value of “0”, as depicted in the first case of Fig. 1 (a), will produce a zero power output signal for an input vector of [Bit=0, $\overline{Bit}$=1], corresponding to a “match” state. Following the same rationale, the respective ON/OFF states of the consituent cells configure the three stored values. Figure 1 (b) shows a close-up miscoscope image of a single UV-exposable MZI. The cell consists of strip waveguides with 1μm width and thickness of 400 nm, being designed for a wavelength of 1550 nm and a TE polarization. Additionally, the waveguide core material is n-rich Si_3N_4 with a refractive index of 1.9 and is deposited using PECVD on a silicon wafer with 3.2 μm of thermally grown oxide, while the waveguide is clad with 2 μm of PECVD SiO_2. The refractive index of the n-rich core is altered through a laser exposure process. A 244 frequency-doubled Argon-Ion laser targets a 14 μm beam

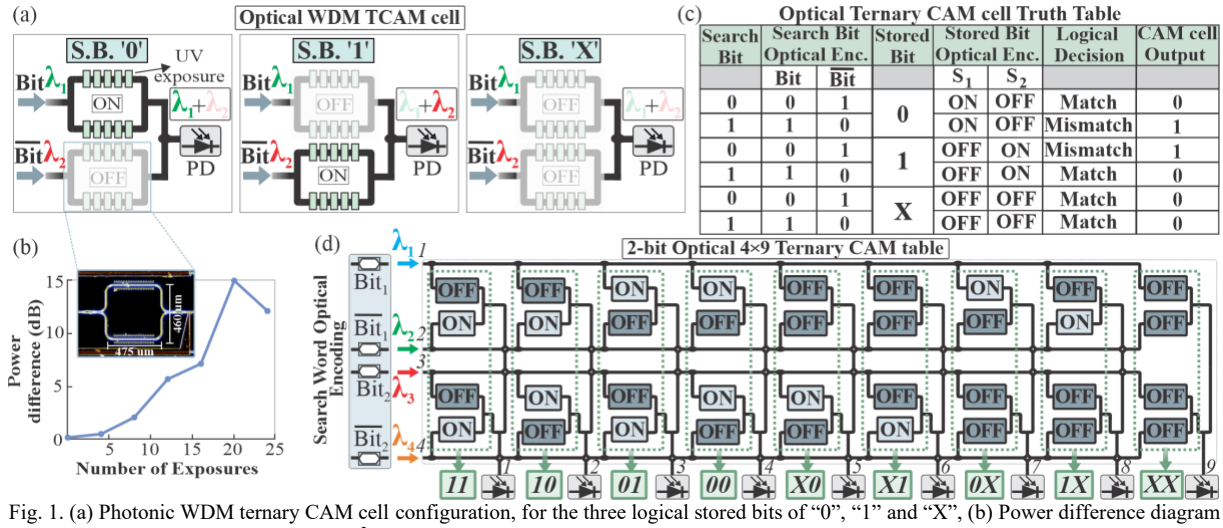

Search Bit	Search Bit Optical Enc.		Stored Bit	Stored Bit Optical Enc.		Logical Decision	CAM cell Output
	Bit	$\overline{Bit}$		S_1	S_2		
0	0	1	0	ON	OFF	Match	0
1	1	0		ON	OFF	Mismatch	1
0	0	1	1	OFF	ON	Mismatch	1
1	1	0		OFF	ON	Match	0
0	0	1	X	OFF	OFF	Match	0
1	1	0		OFF	OFF	Match	0

Fig. 1. (a) Photonic WDM ternary CAM cell configuration, for the three logical stored bits of "0", "1" and "X", (b) Power difference diagram based on the number of exposures (kJ/cm^2), along with a microscope image of the UV-exposable MZI building block (*inset*), (c) Truth table of the ternary CAM cell and (d) Conceptual layout of the 2-bit optical 4×9 WDM TCAM table architecture.

spot on the surface of the photonic integrated structure (PIC). Figure 1 (b) depicts the optical power difference evolution between the starting and final optical power emerging at a Mach Zehnder modulator (MZM) output, after consecutive UV-exposures. Specifically, the raster pattern of one of the arms is exposed by a laser source (typical power of 25 mW) with a fluence of 1.5 kJ/cm^2, with every exposure reducing the refractive index of the n-rich core, thus inducing an additive phase difference between the arms of the interferometer. The ON and OFF states of the cell are then defined at the maximum power difference, specifically the ON state at 0 exposures and the OFF states at 20 exposures where a 15 dB power difference is observed. Finally, it should be noted that the UV-exposure processing steps are wafer-scale compatible highlighting a viable roadmap for mass manufacturing.

In Figure 1 (c) the logical truth table of the TCAM cell is depicted, showing the encoding of all three possible binary and ternary stored combinations, revealing that a "match" emerges when only a TCAM cell output signal equals to the logical "0". Figure 1 (d) presents a 4×9 WDM-based TCAM array, that incorporates all 9 different stored 2-bit words. The architecture utilizes four different wavelengths to encode the different Bit_1, Bit_2 and $\overline{Bit}_1$, $\overline{Bit}_2$ values for the 2-bit search, that are subsequently broadcasted at all nine Xbar columns. The multi-wavelength signal emerging at each Xbar column is then injected into a PD, with the constituent product components summed incoherently. As such, the PD output at each Xbar column will provide a zero-output level for a TCAM table matchline (ML) operation.

3. Experimental Setup and Results

Figure 2 (a) shows a microscope image of the SiPho integrated 4×9 TCAM prototype, comprising 36 UV-exposable MZI building blocks. Figure 2 (b) depicts the experimental setup employed for the evaluation of the 2-bit TCAM comparison operation. Four different tunable laser sources (TLSs) were used to generate continuous wave signals (CWs) at the wavelengths of 1556, 1557, 1558 and 1559 nm, respectively. An arbitrary waveform generator (AWG) was used to produce two NRZ pseudo random sequences (PRBS^9) (Bit_1, Bit_2) at 20 Gb/s and their complementary ones ($\overline{Bit}_1$, $\overline{Bit}_2$). The RF signals were amplified to ~5.5 Vpp and subsequently injected as driving signals at four different $LiNbO_3$ MZM modules. As such, the optical signals emerging at the modulator outputs were inscribed with

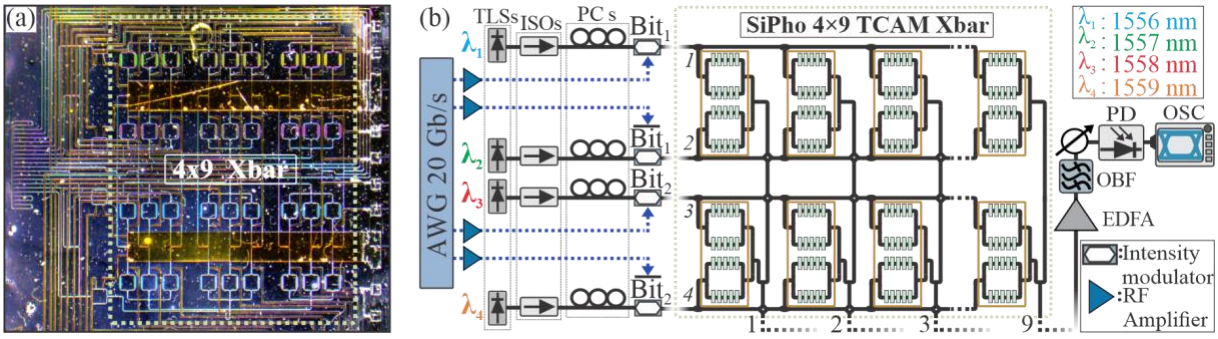

Fig. 2. (a) Microscope image of the WDM 4×9 TCAM photonic crossbar prototype, (b) Experimental setup of the 2-bit TCAM ML operation at 20 Gb/s, the integrated crossbar layout is highlighted (*green*), along with the respective UV-exposed MZI cells of each column (*brown*).

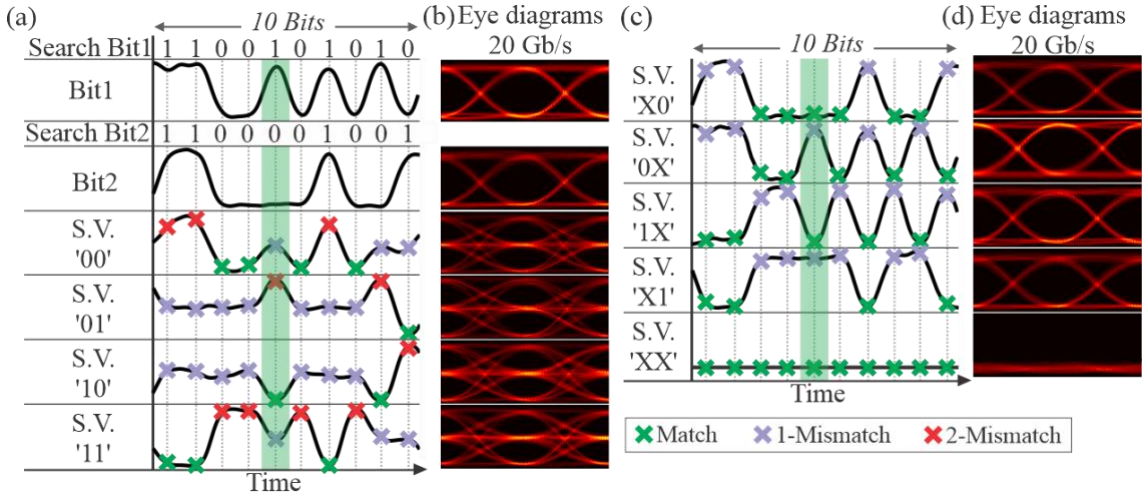

Fig. 3. (a) Synchronized time traces (50 ps/div) of 10 optically encoded search bits (Bit_1, Bit_2) and the binary S.V. cases of "00", "01", "10" and "11", (b) respective eye diagrams for 20 Gb/s. (c) Time traces of the ternary S.V. cases "X0", "0X", "1X", "X1" and "XX", (d) Eye diagrams for ternary cases at 20 Gb/s. The colored scatter points indicate the level of Mismatch of each case.

the produced data sequences, constituting the 2-bit search word information. The four signals were then forwarded through grating couplers into the four input ports of the Xbar array. Each column of the Xbar encoded on of the 9 different 2-bit binary and ternary combinations ("00"- "XX"), based on the exposed states of its constituent weight cells. All signals emerging at the Xbar's outputs were then amplified by an erbium doped fiber amplifier and filtered by a bandpass filter of 4 nm before being acquired by a 70 GHz photodiode and a 75 GHz sampling oscilloscope. Incoherent addition of the multi-wavelength signal emerging at each column output, allowed calculation of the dot-product between the stored and search word. Finally, all signals were processed using a digital signal processing module, comprising a low pass butterworth filter and a linear equalizer. The total loss for every Xbar output/input combination was approximately ~50 dB, mainly dominated by the use of non-optimal grating couplers (GCs) for optical input/output coupling (11.5 dB/GC) and multiple 70/30 monitor ports (~6 dB/monitor) that were employed in this prototype for ease of testing. Considering an approach where on-chip lasers are utilized and the monitors are implemented with a 99/1 splitting ratio, the total losses can be reduced down to approximately 20 dB, with the ~9.5dB stemming from the 1:9 splitting losses.

Figure 3 demonstrates 10-bit sequences of synchronized time traces at 20 Gb/s, of the search Bit_1/Bit_2 and all 9 Xbar outputs representing different stored vectors (S.V.s). Figure 3 (a) shows the search bit time traces along with all the binary S.V. values, while Fig. 3 (c) shows the respective ternary cases. Figure 3 (b) and (d) illustrate all the respective eye diagrams of each case, highlighting clear eye openings for all search and stored cases. The S.V. time sequences are marked with cross-shaped scatter points, with their color indicating the respective "match" or "mismatch" logic state. Specifically, the green highlighted area presents the case of the search word being "10" (Bit_1=1, Bit_2=0). A zero-power level value is produced only in the case of a logical 'match" at the TCAM output, where the search information is identical to the stored case. In the case that a 1-level or 2-level power signal is produced the respective "1-Mismatch" and "2-Mismatch" cases occur. The ternary "X" value produces a constant "match", regardless of the incoming search information. The experimentally acquired signals were also evaluated through a theoretical error rate analysis, revealing error-free operation with values well below 10^{-9} for all cases under study.

4. Acknowledgements

This work has been funded by the European Commission (EC) through projects OCTAPUS (101070009) and AMBROSIA (101093166) as well as EPSRC under grants EP/M013294/1 and EP/W524621/1.

5. References

[1] K. Pagiamtzis et. al., "Content-addressable memory (CAM) circuits and architectures: a tutorial and survey," IEEE JoSS, March 2006.
[2] T. Moschos et. al., Nonlinear Optical Vector Processing using Linear Silicon Photonic Circuits for 50 Gb/s Memory and String Similarity functions, accepted at Nature Communications.
[3] P. R. Prucnal, et. al., "Recent progress in semiconductor excitable lasers for photonic spike processing," Adv. Opt. Photon., 2016.
[4] T. Moschos et. al., "An All-Optical Address Look-Up Table Using Optical CAM and Optical RAM Banks," in JLT, 2022.
[5] Y. London et. al. "Multiplexing in Photonics as a Resource for Optical Ternary Content-addressable Memory Functionality", Nanoph. 2023.
[6] T. Moschos et al., "A 50 Gb/s WDM Silicon Photonic Ternary Content Addressable Memory cell," 2025 OFC.
[7] G. Mourgias-Alexandris, et al., "All-optical 10Gb/s ternary-CAM cell for routing look-up table applications," Opt. Exp. 26, 2018.
[8] Greta De Paoli, et.al., "Laser trimming of the operating wavelength of silicon nitride racetrack resonators," Photon. Res. 8, 677-683 (2020).
[9] F. Gardes, et al. A Review of Capabilities and Scope for Hybrid Integration Offered by Silicon-Nitride-Based Photonic Integrated Circuits. *Sensors*, 2022.